Received: November 30, 2018
Revised: December 29, 2018
Accepted: December 30,2018

Thai J. Nanosci. Nanotechnol. Volume 3. Issue 2. (2018)

Investigation of Metal Electrode Effect on Electrical Conductivity of $[KNbO_3]_{0.9} - [BaNi_{0.5}Nb_{0.5}O_3]_{0.1}$ Ceramics by Impedance Spectroscopy

Saichon Sriphan[1,2,3,8*], Naratip Vittayakorn[3,4], Mati Horpratum[5], Sasiporn Prasertpalichat[6,7], Theerachai Bongkarn[6,7] and Suwit Kiravittaya[8]

[1]*Department of Telecommunication Engineering, Faculty of Engineering and Architecture, Rajamangala University of Technology Isan, Nakhon Ratchasima 30000, Thailand*

[2]*Aviation Industrial Institute, Rajamangala University of Technology Isan, Nakhon Ratchasima 30000, Thailand*

[3]*Advanced Material Research Unit, Faculty of Science, King Mongkut's Institute of Technology Ladkrabang, Bangkok 10520, Thailand*

[4]*Department of Chemistry, Faculty of Science, King Mongkut's Institute of Technology Ladkrabang, Bangkok 10520, Thailand*

[5]*National Electronics and Computer Technology Center, Thailand Science Park, Pathumthani 12120, Thailand.*

[6]*Research Center for Academic Excellent in Applied Physics, Faculty of Science, Naresuan University, Phitsanulok 65000, Thailand*

[7]*Department of Physics, Faculty of Science, Naresuan University, Phitsanulok 65000, Thailand*

[8]*Advanced Optical Technology Laboratory, Department of Electrical and Computer Engineering, Faculty of Engineering, Naresuan University, Phitsanulok 65000, Thailand*

Abstract

Perovskite ceramic of $[KNbO_3]_{0.9} - [BaNi_{0.5}Nb_{0.5}O_3]_{0.1}$ (KBNNO) was fabricated using the solid-state combustion technique. KBNNO was sandwiched among different metal electrodes to investigate the electrical conductivity behavior. From the impedance spectroscopy, the dispersion of impedance curves was found with the increase of frequency as well as heating temperature. This observation indicated that KBNNO ceramic exhibits dielectric relaxation phenomenon. The equivalent grain resistance value obtained from the impedance analysis significantly decreased after changing the electrode from indium tin oxide (ITO) to Ag, indicating the influence of active electrode on ceramic conductivity. The possible reason was due to the low resistivity of Ag electrode as compared with ITO. This suggested that the electrical charge would easily transfer to external load. The presented results were essential for making a new route to investigate the electrical properties of KBNNO-based material, and further develop novel electroceramics.

Keywords: KBNNO; Metal Electrode; Impedance Spectroscopy; Equivalent Circuit Model

1. Introduction

Since the first discovery of a perovskite $BaTiO_3$ (BT) in the 1940s [1], a study of various oxide perovskite ceramics has gained a lot of interest. Among the studied ferroelectric oxide ceramics, $Pb(Zr,Ti)O_3$ (PZT) is outstanding material. It provides the excellent properties, i.e., good dielectric constant (ε_r ~2000), high piezoelectric coefficient d_{33} (~200 – 750 pC/N), etc., in which suitable for electronic devices fabrication [2-5]. However, due to the toxic nature of PZT, searching for new lead-free ferroelectric ceramic is essential to replace a lead-based material without losing the physical properties required for device development. $(K_{0.5}Na_{0.5})NbO_3$ (KNN) is one of such lead-free ferroelectric $KNbO_3$ (KN)-based ceramics. The engineered KNN ceramics achieves d_{33} of ~425 – 570 pC/N with a rhombohedral-

Corresponding Author E-mail: saichon.sr@rmuti.ac.th

tetragonal phase coexistence [5]. This property is in the same trend as the PZT, indicating the promising candidate to replace a PZT ceramic. For the family of KN-based ceramics, a recent developed $[KNbO_3]_{1-x} - [BaNi_{0.5}Nb_{0.5}O_{3-\delta}]_x$ ($KBNNO_x$), where δ is the oxygen deficiency, is interesting. The highest ferroelectric properties are found at the compositions of $x = 0.1$ and $\delta = 0.25$. The capability of this ceramic is to tune many properties such as optical, dielectric, piezoelectric, pyroelectric and magnetic ones [6-8]. Owing to these properties, $KBNNO_x$ can be used to make a multi-functional device or utilizing together with other materials.

Impedance spectroscopy (IS) is a powerful tool to investigate the electrical properties of electroceramics [9-15]. It enables the evolution of internal responses of bulk, grain boundary and electrode interface effects in the relaxation frequency of materials. This technique has successfully been used for studying various kinds of electroceramics, for example, BT [11], KNN [12], $0.85[(1-x)Bi_{0.5}Na_{0.5}TiO_3 - xBaTiO_3] - 0.15Na_{0.73}Bi_{0.09}NbO_3$ [13] and $(Bi_{1.5}Zn_{0.5})(Nb_{0.5}Ti_{1.5})O_7$ [14], by focus on electrical conductivity at elevated temperatures. However, until now, the mechanism of electrical conductivity studied by IS technique of $KBNN_x$-based ceramic has not yet been reported.

Herein, $KBNNO_x$ was designed to enhance the dielectric properties by setting $x = 0.1$ and $\delta = 0$, which was $[KNbO_3]_{0.9} - [BaNi_{0.5}Nb_{0.5}O_3]_{0.1}$ (KBNNO) [16,17]. During ceramic synthesis, the solid-state combustion (SSC) technique was used. The added fuel used for combustion effectively speeds up the chemical reaction. High quality of ceramics is finally obtained with lower sintering temperature and a shorter dwell time [16-18]. The effects on the microstructure and dielectric properties were investigated. The IS technique was applied to investigate the electrical conductivity of KBNNO. Due to a rare report of electrode effect on the electrical conductivity of electroceramics, thus, this work also investigated this effect on KBNNO ceramic.

2. Experimental details

The solid-state combustion (SSC) method was used to prepare KBNNO ceramics. The precursors of KNO_3, $Ba(NO_3)_2$, NiO and Nb_2O_5 were weighted in their stoichiometric proportions. The nitrates and oxides were mixed in ethanol and ball-milled for 24 h. A glycine ($C_2H_5NO_2$), as an activator for the SSC method, was mixed with the dried powders at 1:0.61 ratio. The mixed powders were calcined in an electrical furnace at 650°C for 1.5 h to form the perovskite phase [16]. After that, the calcined powders (1.2 g) was pressed at ~197 MPa into pellets with a diameter of 15 mm and about 1.2 mm in thickness. The KBNNO pellets were then sintered at 1100°C for 3 h in air atmosphere, similar to our previous work [17]. Various kinds of electrodes, i.e., indium tin oxide (ITO), platinum (Pt) and silver (Ag), were applied on the KBNNO surface to investigate the ceramic conductivity. The coating of ITO on KBNNO surface was achieved by using an ion-assisted electron-beam evaporation (DENTON-DVB SJ-26C) inside the vacuum (base pressure of 2.3×10^{-6} Torr) with the source materials of ITO pellets (99.99% purity). The KBNNO ceramic was cleaned by acetone and then dried with nitrogen gas. Prior to the thin film deposition, the ceramic was cleaned in argon (Ar) plasma at 20 sccm for 5 minutes to remove the surface contamination. The deposition chamber was operated at 100 W with the operated pressure of 1.9×10^{-6} Torr. The ITO thickness was constantly controlled to be 150 nm. In addition, the Pt and Ag electrodes were deposited on KBNNO ceramic surface using a pulsed dc reactive magnetron sputtering (AJA International, Inc., ATC 2000-F). The KBNNO was cleaned by acetone and dried in nitrogen atmosphere. After that, the ceramic was cleaned in vacuum chamber (5×10^{-3} Torr)

by Ar plasma for 5 minutes in the rate of 20 sccm in order to remove the surface contamination. The UHV deposition chamber with the base pressure of 1×10^{-6} operated at 100 W was used. The nanostructured Pt and Ag films were grown by maintaining the thickness to be the same as ITO.

To confirm the phase purity and structure of KBNNO ceramic, x-ray diffraction (XRD, PANalytical X'Pert PRO) technique was used. Field emission scanning electron microscopy (FESEM, JSM-7001F) was taken to observe the ceramic surface. The density of ceramic was determined by the Archimedes method. The ε_r and loss tangent tan δ were recorded using LCR meter (Agilent 4263B) with a heater (measured at room temperature to 400°C). Impedance spectroscopy measurement was carried out by using Keysight impedance gain/phase analyzer (model 4194A). The IS data was measured at the heating temperatures between 400°C and 500°C (25°C /step) and the frequencies ranging from 20 Hz to 1 MHz with an operating AC voltage of 0.1 V. Measurements were recorded in air atmosphere to investigate the spectroscopic plots of the real part (Z′) and imaginary part (Z″) of the impedance data.

3. Results and discussion

The Fig. 1(a) shows the room temperature XRD pattern (2θ range of 10° - 60°) of KBNNO sintered at 1100°C for 3 h. The perovskite peaks were observed without any additional impurity phases. This indicated a high purity of the fabricated ceramic. Main diffraction perovskite peaks, i.e., (001), (110), (200), (210) and (211), of KBNNO ceramic matched with the standard cubic $KNbO_3$ (KNO) *Pm3m* structure in JCPDS file no. 08-0212. The surface morphology of KBNNO is shown in an inset of Fig. 1. Fully dense structure with average grain size of ~117 ± 11 nm was clearly evidenced. To investigate the physical property of the fabricated ceramic, the percentage of theoretical density (%T.D.) was calculated. This factor can be determined by using a percentage of the measured ceramic density *D* divided by the theoretical density. For our KBNNO ceramic, the measured *D* was approximately 4.80 g/cm^3. The obtained *D* was higher than many KNO-based ceramics such as $K_{0.5}Na_{0.5}NbO_3$ [19] and MnO_2 doped with $(K_{0.5}Na_{0.5})_{0.94}Li_{0.06}NbO_3$ [20]. The calculated theoretical density was 4.88 g/cm^3 [7,8]. A high value of *D*, which provided the %T.D. of about 98.36%, was due to the application of ball-milling and use of SSC technique in the ceramic fabrication process. The effective of using these techniques was that the aggregated particles could be dispersed causing a compact ceramic before sintering in the furnace.

Generally, there is the relation of *D* among ε_r, tan δ and electrical conductivity of electroceramics. For the couple of *D* and ε_r, the change of grain size and the reduction in the total grain boundary are observable due to the grain growth during sintering process [21,22]. With the increase of sintering temperature, many distinctive pores are found, and they tend to decrease while grains are growing. In the optimum sintering temperature, high density ceramic is obtained, coherently leading to a high value of ε_r. Additionally, a main mechanism of dielectric loss (or tan δ) is an electric charge migration [22]. Large amount of porosity causes a high value of tan δ because the incoming charges can be easily migrated throughout the ceramic. For electrical conductivity of ceramic, when the ceramic material has a higher density, the electrical conductivity of ceramic tends to increase [23,24]. This is due to the raise of electron density during sintering process [24]. Hence, understanding these relations is essential in which could alter the ceramic properties for being used in the certain application.

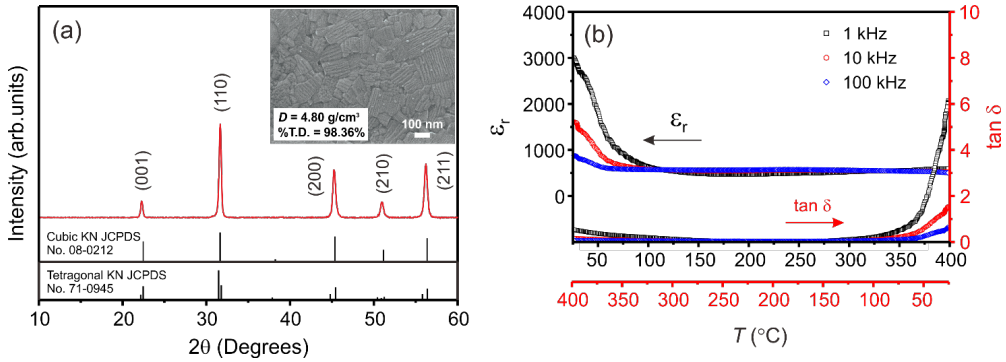

Fig. 1. (a) XRD pattern of KBNNO sintered at 1100ºC for 3 h. Inset shows the scanning electron microscopy (SEM) image of KBNNO ceramic. (b) Temperature dependence of the dielectric properties of KBNNO ceramic recorded at 1, 10 and 100 kHz.

The variations of ε_r and tan δ with heating temperatures for KBNNO ceramic are shown in Fig. 1(b). All data were recorded from 25°C to 400°C at three operating frequencies of 1, 10 and 100 kHz. It has been observed that, over 100°C, KBNNO showed the stable values of ε_r and tan δ. The variation of these data with different frequencies was seen at low temperature (< 100°C). This indicated a low value of Curie-Weiss temperature T_C, which affected the phase transition of our KBNNO ceramic [25]. The anomalous result might be due to the adding of $BaNi_{0.5}Nb_{0.5}O_3$ into KNO structure [6]. The highest ε_r of ~3000 was found at 1 kHz. The obtained ε_r of our samples was higher than the typical $KBNNO_x$ and the classical KNO by about 5 times [6] and 3 times [26], respectively. Nevertheless, a high value of tan δ (~6 at 1 kHz) was observed. Typically, the main mechanism of dielectric loss is ion migration, which is strongly affected by temperature, especially around T_C [22]. Hence, a high dissipation loss in this case was caused by a high internal porosity of KBNNO that should be focused to improve in the further work.

The IS analysis is an effective way to investigate the electrical and dielectric properties of materials [9-15]. The influence of different active electrodes on the impedance value of KBNNO ceramic was conducted using the IS technique. Four series of KBNNO structure were designed by sandwiching KBNNO ceramic with different metal electrodes. In this case, the top surface was fixed with the ITO electrode, while other active electrodes at the bottom were varied. The designed structures were ITO/KBNNO/ITO (S1), ITO/KBNNO/Pt (S2) and ITO/KBNNO/Ag (S3). The frequency dependences of Z′ and Z″ in each series are shown in Figs. 2 and 3. These data were measured at the frequencies ranging between 20 Hz and 1 MHz with the controlled heating temperatures from 400°C to 500°C. For Z′ results (Fig. 2), the magnitudes of Z′ for all series tended to decrease when frequency increased. The decrease of Z′ data was a lowering of material barrier properties [11]. This leaded to an increase of electrical conductivity at elevated frequency. Variation of Z′ magnitude could be observed incessantly until 100 kHz followed by a saturation region above this frequency. The saturation phenomenon was due to the complete mixed natures of material polarization [12]. With increase the heating temperature from 400°C to 600°C, the magnitude of Z′ significantly decreased especially at the frequency below 1 kHz. However, the tendency of Z′ value was contrary when the frequency was higher. There was a turning point of Z′ value around 1 kHz. The possible reason to explain the reduction of Z′ value with the increase of heating temperature was the presence of negative temperature coefficient resistance in the material [11]

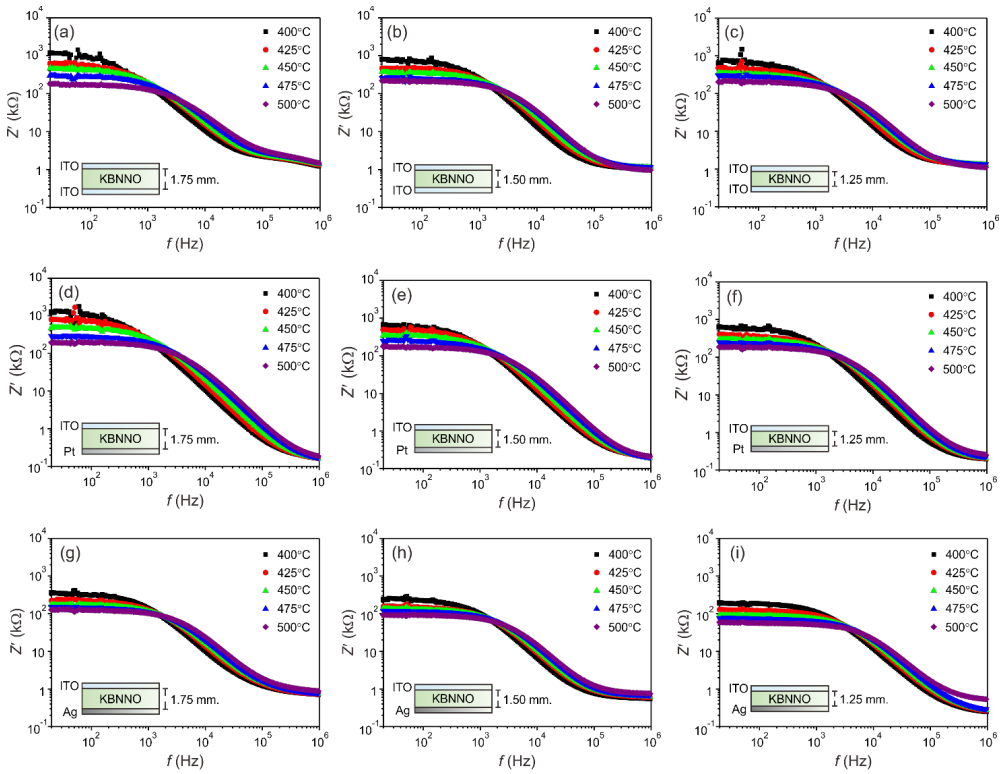

Fig. 2. Real part of impedance (Z′) with frequency variation for KBNNO ceramics fabricated in different structures: (a - c) ITO/KBNNO/ITO, (d - f) ITO/KBNNO/Pt and (g - i) ITO/KBNNO/Ag at various heating temperatures. Inset shows the corresponding schematic of the fabricated samples.

[11]. The merging of all curves at higher frequency suggested the occurrence of releasing space charge and lowering of material barrier properties [11]. When one reduced the KBNNO thickness (1.75 mm to 1.25 mm) for all device structures, the magnitude of Z′ systematically decreased. This was typical because the ceramic resistivity reduced, leading to an enhancement of its conductivity. Interestingly, with the change of bottom electrodes (ITO, Pt and Ag), the obvious reduction of Z′ value was observable. By changing ITO to Pt (S2 sample), there was nothing different on the Z′ value (~1 MΩ). Not much change of the impedance data on ITO and PT electrodes was because of the rather similar of their electrical resistivity, which are 7.20×10^{-6} Ω·m for ITO [27] and 1.06×10^{-7} Ω·m for Pt [28]. Therefore, the amount of transferred charges was no different. However, the Z′ reduction about half was seen after changing the bottom electrode from ITO to Ag (S3 sample). This was due to a much lower electrical resistivity of Ag (around 1.59×10^{-8} Ω·m) [28], inducing more transferred electric charges to the external load. This effect thus caused the numerous reduction of the Z′ value for S3 sample.

Figure 3 shows the frequency dependence of Z″ spectra at various heating temperatures for KBNNO ceramic. In the same manner as Z′ results (Fig. 2), the decrease of Z″ in different bottom electrodes could be observed for all conditions of heating temperature and thickness. By changing ITO to Ag electrode (S3 sample), the Z″ data reduced about half as rather similar

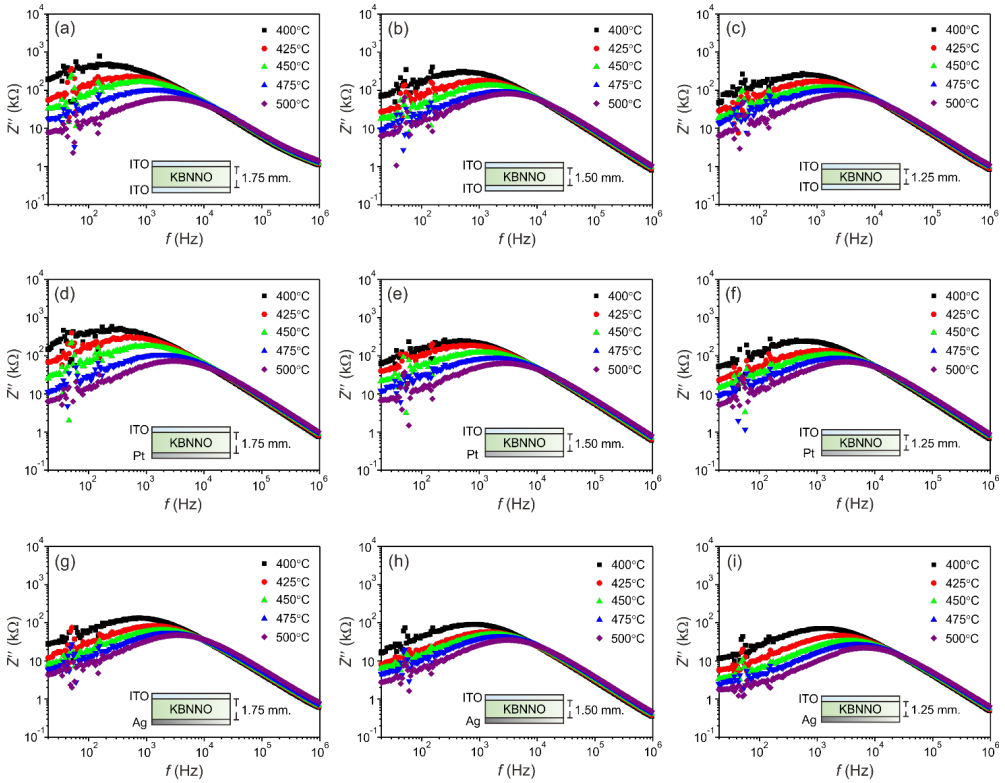

Fig. 3. Imaginary part of impedance (Z″) with frequency variation for KBNNO ceramics fabricated in different structures: (a - c) ITO/KBNNO/ITO, (d-f) ITO/KBNNO/Pt and (g - i) ITO/KBNNO/Ag at various heating temperatures. Inset of each figure shows a schematic of the investigated sample.

to the decrease of Z′. The obtained results were considered at the frequency below 1 kHz, while at the higher frequency, the Z″ data curves tended to merge. The decrease of both Z′ and Z″ data leaded to the substantial decrease of semicircular area of Cole-Cole plot, as shown below in Fig. 4. The frequency dependence of Z″ indicated the influence of an electrical relaxation process in the material [9,11]. The shift of impedance peaks implied the decrease of a net relaxation time with temperature raised [11,12]. The dispersive nature in the Z″ spectra demonstrated the presence of electronic, dipolar and space charge polarizations at low-frequency region. From these results, it could be confirmed that our KBNNO behaved a relaxor ferroelectricity [14].

Figure 4 reveals the plots of Z′ versus Z″, as called Nyquist or Cole-Cole plots, at different heating temperatures. The plot results obtained from the data of Figs. 2 and 3. Only one semicircular arc was observed, which associated with the bulk response of ceramic [9,10,12]. With the increase of heating temperature, the obtained arc features for all conditions were not different, i.e., they still showed only a single semicircle arc. This indicated the physical mechanism inside KBNNO ceramic was not change much at elevated temperatures. Smaller semicircle, i.e., area under the curves decreased, was observed during the temperature increased. Generally, the semicircle arc can be theoretically expressed in term of an equivalent

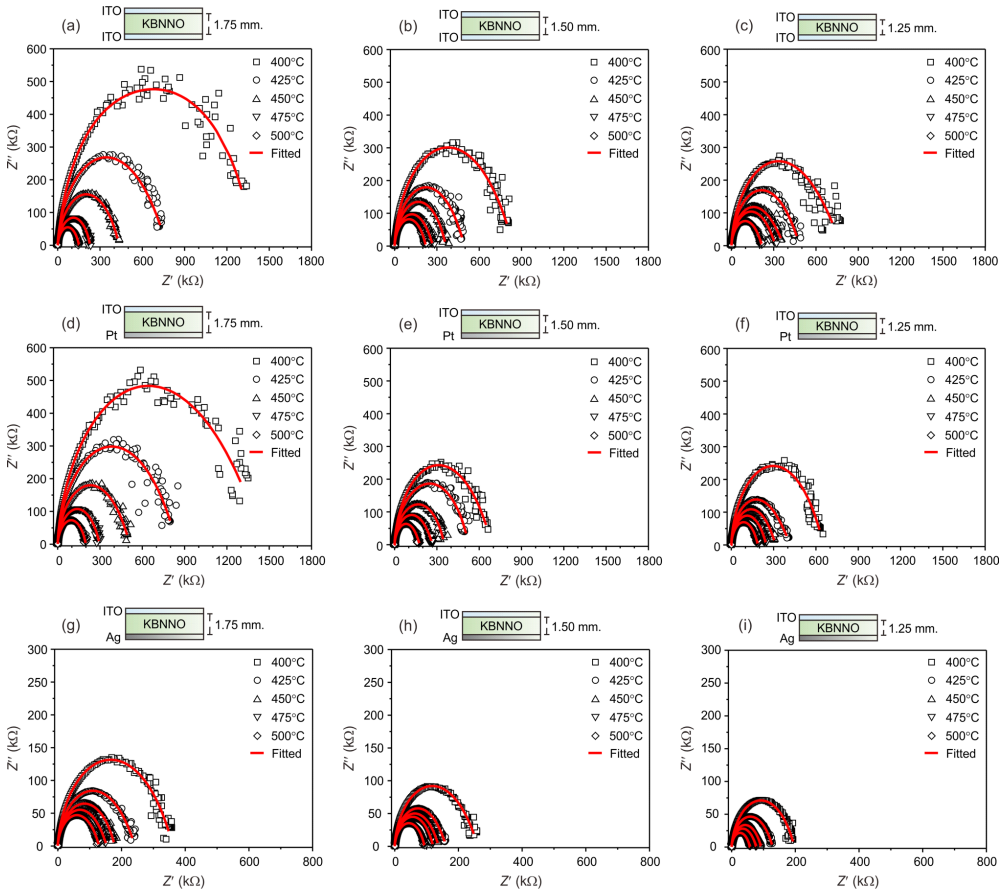

Fig. 4. Nyquist plots (Z′ - Z″) plotted with the fitted spectra (red solid lines) for KBNNO samples fabricated in different structures: (a - c) ITO/KBNNO/ITO, (d-f) ITO/KBNNO/Pt and (g - i) ITO/KBNNO/Ag at various heating temperatures.

circuit. Hence, we had fitted the experimental data using EC-Lab software for all samples by the equivalent circuit model proposed in Fig. 5(a). This circuit consists of a resistor, as represented to a grain resistance R_G, in parallel with a capacitor, as represented to a grain capacitance C_G. We found that the circuit included only the parallel R_GC_G could not model the recorded semicircle arc. In this case, the series connection of a trap resistance R_{trap} and a constant phase element *CPE* was also parallel together with R_G and C_G. The *CPE* expresses an ideal resistor (n = 0) and an ideal capacitor (n = 1) in the representation of electrical admittance: $Y_{CPE} = A_0(j\omega)^n = A\omega^n + jB\omega^n$, where $A = A_0\cos(n\pi/2)$ and $B = A_0\sin(n\pi/2)$. For this equation, A_0 and n are temperature dependent but frequency independent parameters, meaning that Y_{CPE} factor would change with the rising of heating temperature [13-15]. There were two mechanisms behind the proposed circuit (Fig. 5(a)): the R_G and C_G contributed the grain (bulk) response, and the $R_{trap}CPE$ series would represent the contribution of electron trap (called electron trap section). The addition of electron trap section was required to provide the best fit of the measured impedance data, and became the factor used to explain the trap state in material [10]. The fitted results were shown in Fig. 4. It has been seen that there was a close

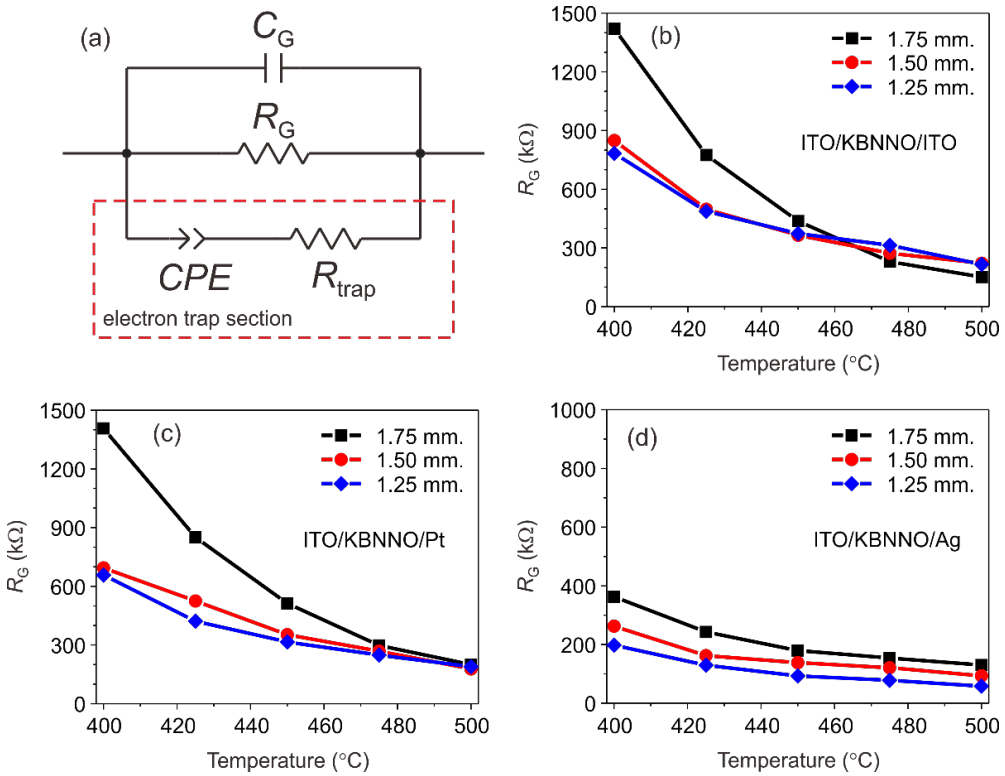

Fig. 5. (a) Possible equivalent circuit used to fit the impedance spectra. (b - d) Variations of grain resistance R_G with heating temperatures of KBNNO samples for (b) ITO/KBNNO/ITO, (c) ITO/KBNNO/Pt and (d) ITO/KBNNO/Ag structures, respectively, in the difference of KBNNO thicknesses.

agreement between the observed and fitted data. Figs. 5(b) - (d) display the fitted R_G parameters for all samples. The obtained R_G values corresponded to the intercept of the semicircle in the complex impedance plane on the real axis. We found that R_G systematically decreased with the rise of heating temperature and the decrease of ceramic thickness. These effects might be related to the microstructural change of material during thermal state (thermal activated process), which suggested the relation between electrical properties and thermal-dependent microstructure of material [12]. Since the bottom electrode was changed from ITO to Ag (S3 sample), the R_G substantial decreased for all conditions, which was consistent with the previous Z′ and Z″ data (Figs. 2 and 3). The reduction of R_G for the change of electrode clearly indicated the role of more conductive electrode that was able to enhance the conductivity of KBNNO ceramic.

4. Conclusion

The $[KNbO_3]_{0.9} - [BaNi_{0.5}Nb_{0.5}O_3]_{0.1}$ (KBNNO) has been synthesized by the solid-state combustion technique with the sintering temperature of 1100°C for 3 h. Using FESEM, we observed a compact structure of KBNNO ceramic, with $d = 4.80$ g/cm^3 (98.36% of %T.D.). This was higher than a reference $KBNNO_x$ designed for $\delta = 0.25$ and a classical $KNbO_3$ by about 5 times and 3 times, respectively. The way to achieve a high density was using the ball

milling technique to reduce the particle size before sintering process. A high ε_r of ~3000 was found and a high dissipation loss (tan δ ~ 6 at 1 kHz) was also observable. The latter was due to the effect of internal porosity. Electrical properties of KBNNO at various structures realized by different metal electrodes, i.e., ITO, Pt and Ag, have been investigated. Real and imaginary parts of impedance data for all samples obeyed a continuous dispersion with the increase of frequency and heating temperature. This revealed the dielectric relaxation process in KBNNO ceramic. It has been found that the impedance data could reveal the effect of bottom electrode change on the electrical conductivity of KBNNO. By changing the bottom electrode from ITO to Ag, real and imaginary impedances significantly decreased (approximately half). The Cole-Cole curves also showed in the same impedance reduction trend as the Z′ and Z″ data. These curves were fitted with the circuit composed of a resistor, as represented to a grain resistance, in parallel with a capacitor, as represented to a grain capacitance. The proposed resistance and capacitance elements were connected together with an electron trap section, which consisted of a trap resistance and a constant phase element. This was to provide the best fit of the Cole-Cole plots. The decrease of the impedance data after bottom electrode change was might be due to Ag has much lower resistivity than ITO. Hence, the present work revealed a new route to investigate the electrical properties of $KBNNO_x$-based material by IS technique. The role of enhancing the amount of charge transfer was also suggested by changing a higher resistivity of an active electrode to be lower, which was finally able to reduce the internal ceramic resistance.

Acknowledgement

This work is financially supported by Naresuan University and the Faculty of Engineering, Naresuan University. The work of N.V. was supported by faculty of Science, KMITL under grant no 2562-01-05-46.

References

[1] Uchino K. Ferroelectric Devices. New York, USA: Marcel Dekker Inc.; 2000.
[2] Maeder MD, Damjanovic D, Setter N. Lead free piezoelectric materials. J. Electroceramics. 2004;13(1-3):385-392.
[3] Jaffe B, Cook JWR, Jaffe H. Piezoelectric Ceramics. London, England: Academic Press.; 1971.
[4] Saito Y, Takao H, Tani T, Nonoyama T, Takatori K, Homma T, Nagaya T. Nakamura M. Lead-free piezoceramics, Nature. 2004;432:84-87.
[5] Wu J, Xiao D, Zhu J. Potassium-Sodium Niobate Lead-Free Piezoelectric Materials: Pass, Present, and Future of Phase Boundaries. Chem. Rev. 2015;115(7):2449-2595.
[6] Grinberg I, West DV, Torres M, Gou G, Stein DM, Wu L, Chen G, Gallo EM, Akbashev AR, Davies PK, Spanier JE, Rappe AM. Perovskite oxides for visible-light-absorbing ferroelectric and photovoltaic materials. Nature. 2013;503:509-512.
[7] Zhou W, Deng H, Yang P, Chu J. Structural phase transition, narrow band gap, and room-temperature ferromagnetism in $[KNbO_3]_{1-x}$ $[BaNi_{1/2}Nb_{1/2}O_{3-\delta}]_x$ ferroelectrics. Appl. Phys. Lett. 2014;105(11):111904.
[8] Bai Y, Siponkoski T, Perantie J, Jantunen H, Juuti J. Ferroelectric, pyroelectric, and piezoelectric properties of a photovoltaic perovskite oxide. Appl. Phys. Lett. 2017;110 (6):063903.
[9] Irvine JTS, Sinclair DC, West AR. Electroceramics: characterization by impedance spectroscopy. Adv. Mater. 1990;2(3):132-138.

[10] Schipani F, Miller DR, Ponce MA, Aldao CM, Akbar SA, Morris PA. Electrical characterization of semiconductor oxide-based gas sensors using impedance spectroscopy: a review. Rev. Adv. Sci. Eng. 2016;5(1):86-105.
[11] Wang Y, Pu Y, Zhang P. Investigation of dielectric relaxation in $BaTiO_3$ ceramics modified with $BiYO_3$ by impedance spectroscopy. J. Alloys Compd. 2015;653:596-603.
[12] Rai R, Coondoo I, Rani R, Bdikin I, Sharma S, Kholkin AL. Impedance spectroscopy and piezoresponse force microscopy analysis of lead-free $(1-x)K_{0.5}Na_{0.5}$ NbO_3 – $x$$LiNbO_3$ ceramics. Curr. Appl. Phys. 2013;13(2):430-440.
[13] Xu Q, Lanagan MT, Huang X, Xie J, Zhang L, Hao H, Liu H. Dielectric behavior and impedance spectroscopy in lead-free BNT-BT-NBN perovskite ceramics for energy storage. Ceram. Int. 2016;42(8):9728-9736.
[14] Osman RAM, West AR. Electrical characterization and equivalent circuit analysis of $(Bi_{1.5}Zn_{0.5})(Nb_{0.5}Ti_{1.5})O_7$ pyrochlore, a relaxer ceramic. J. Appl. Phys. 2011;109:074106.
[15] Barick BN, Choudhary RNP, Pradhan DK. Dielectric and impedance spectroscopy of zirconium modified $(Na_{0.5}Bi_{0.5})TiO_3$ ceramics. Ceram. Int. 2013;39(5):5695-5704.
[16] Sriphan S, Kiravittaya S, Bongkarn T. Effects of calcination temperature on the synthesis of $[KNbO_3]_{0.9}$ – $[BaNi_{0.5}Nb_{0.5}O_3]_{0.1}$ perovskite powders. Integr. Ferroelectr. 2017;177(1) :112-120.
[17] Sriphan S, Vittayakorn N, Kiravittaya S, Bongkarn T. Microstructural, dielectric and optical properties of $[KNbO_3]_{0.9}$ – $[BaNi_{0.5}Nb_{0.5}O_3]_{0.1}$ perovskite ceramics. IOP J. Phys. Conf. Ser. 2018;1144:012018.
[18] Wattanawikkam C, Vittayakorn N, Bongkarn T. Low temperature fabrication of lead-free KNN-LS-BS ceramics via the combustion method. Ceram. Int. 2013;39(1):S399-S403.
[19] Singh R, Patro PK, Kulkarni AR, Harendranath CS. Synthesis of nanocrystalline potassium sodium niobite ceramic using mechanochemical activation. Ceram. Int. 2014;40(7):10641-10647.
[20] Hao J, Xu Z, Chu R, Zhang Y, Li G, Yin Q. Effects of MnO_2 on phase structure, microstructure and electrical properties of $(K_{0.5}Na_{0.5})_{0.94}Li_{0.06}NbO_3$ lead-free ceramics. Mater. Chem. Phys. 2009;118(1):229-233.
[21] Reed JS. Principles of Ceramic Processing. New York: John Wiley & Sons.;1989.
[22] Richerson DW. Modern Ceramic Engineering: Properties, Processing, and Use in Design. 3rd ed. New York, USA: Taylor & Francis.; 2006.
[23] Niwa E, Uematsu C, Hashimoto T. Sintering temperature dependence of conductivity, porosity and specific surface area of $LaNi_{0.6}Fe_{0.4}O_3$ ceramics as cathode material for solid oxide fuel cells—Superiority of Pechini method among various solution mixing processes. Mater. Res. Bull. 2013;48(1):1-6.
[24] Sedky A, El-Brolossy TA, Mohamed SB. Correlation between sintering temperature and properties of ZnO ceramic varistors. J. Phys. Chem. Solids. 2012;73(3):505-510.
[25] Dong L, Stone DS, Lakes RS. Dielectric and viscoelastic properties of $KNbO_3$ doped $BaTiO_3$. J. Appl. Phys. 2011;109(6):063531.
[26] Krad I, Bidault O, Said S, Saviot L, Maaoui MEL. Phase transitions and dielectric properties of $(1-x)KNbO_3$ – $xK_{0.5}Bi_{0.5}TiO_3$ ceramics synthesized by a stirred hydrothermal process. Curr. Appl. Phys. 2015;15(11):1370-1376.
[27] Chen Z, Li W, Li R, Zhang Y, Xu G, Cheng H. Fabrication of highly transparent and conductive indium-tin oxide thin films with a high figure of merit via solution processing. Langmuir. 2013;29(45):13836-13842.
[28] Serway RA. Principles of Physics. 2nd ed. London, England: Saunders College Publication.; 1998.